Hennadii V. Pavlov
Павлов Геннадий Викторович

Iryna L. Vinnychenko
Винниченко Ирина Леонидовна

УДК 621.314
П12

THE MATHEMATICAL MODEL OF RESONANT FREQUENCY CONVERTER WITH PULSE REGULATION

МАТЕМАТИЧНА МОДЕЛЬ РЕЗОНАНСНОГО ПЕРЕТВОРЮВАЧА ЧАСТОТИ З ІМПУЛЬСНИМ РЕГУЛЮВАННЯМ

DOI 10.15589/SMI. 2018.01.03

Hennadii V. Pavlov Г. В. Павлов, д-р. техн. наук, проф.
gennadiy.pavlov@nuos.edu.ua
ORC ID: 0000-0002-4937-1828

Iryna L. Vinnychenko І. Л. Вінниченко, асп.
i.l.vinnychenko@gmail.com
ORC ID: 0000-0002-3768-1060

Admiral Makarov National University of Shipbuilding, Nikolaev

Національний університет кораблебудування імені адмірала Макарова, м. Миколаїв

Abstract. On the basis of the state variables method, the mathematical model of the resonant converter is constructed, within which the analytical dependences are obtained, which allow calculating the durations of the inter-commutation stages, the certain sequence of which provides the sinusoidal shape of the carrier pulses. The article aim is to study electromagnetic processes in the power section of the resonant frequency converter with pulse control and to obtain the analytical expressions for the durations of the inter-commutative stages of the converter operation. With the usage of the state variables method, the solutions of vector-matrix equations, which describe the processes in the power section of the resonant frequency converter, were obtained. That made possible to get the exact shape of the resonant voltage and current pulses and determine the durations of the inter-commutation stages, which provide their shape, characterized with the low THD. The phase characteristic of the converter operation cycle is constructed as well. The results of the research can be applied in the development of the pulse frequency converters control systems. The obtained analytical expressions allow computing the required switching moments of the converter power transistors.
Keywords: frequency converter; resonant inverter; mathematical model; state variables method; phase characteristics.

Анотація. Отримано аналітичні залежності для розрахунку тривалості міжкомутаційних етапів та моментів їх завершення з метою забезпечення синусоїдальної форми несучих імпульсів напруги на резонансному конденсаторі із низьким коефіцієнтом гармонік. Побудовано фазову діаграму циклу роботи резонансного інвертора з імпульсним регулюванням та проаналізовано електромагнітні процеси в силовій частині перетворювача. Проведено імітаційне моделювання його роботи та побудовано спектр несучих імпульсів напруги на резонансному конденсаторі та імпульсів струму в резонансному контурі.
Ключові слова: дволанковий перетворювач частоти; резонансний інвертор; математична модель; метод змінних стану; фазові діаграми.

Аннотация. Получены аналитические зависимости для расчета продолжительности межкоммутационных этапов и моментов их завершения с целью обеспечения синусоидальной формы несущих импульсов напряжения на резонансном конденсаторе с низким коэффициентом гармоник. Построена фазовая диаграмма цикла работы резонансного инвертора с импульсным регулированием и проанализированы электромагнитные процессы в силовой части преобразователя. Проведено имитационное моделирование его работы и построен спектр несущих импульсов напряжения на резонансном конденсаторе и импульсов тока в резонансном контуре.
Ключевые слова: двухзвенный преобразователь частоты; резонансный инвертор; математическая модель; метод переменных состояния; фазовые диаграммы.

References

[1] Pavlov G. V., Obrubov A. V., Vinnichenko I. L. *Elektromagnitnye protsessy i parametry nakopitelnyh elementov v rezonansnom invertore s nelineynym regulirovaniem* [Electromagnetic processes and storage elements parameters of the resonant inverter with nonlinear control]. Shipbuilding and Marine Infrastructure, Nikolaev, 2015, no. 2(4), pp. 96 – 107.

[2] Sigorskiy V. P. *Matematicheskiy apparat inzhenera* [The mathematical apparatus of the engineer]. Kyiv: "Tekhnika", 1977, 768 p.

[3] Yurchenko O.M., Hutsaliuk V. Ya., Herasymenko P. Yu., Sliesarevskyi I. O. *Model rezonansnoho tranzystornoho invertora napruhy z nyzkochastotnoiu impulsnoiu moduliatsiieiu* [Model of the resonant transistor voltage inverter with low-frequency pulse modulation]. "Technical Electrodynamics", no. 1, 2011, pp. 24 – 30.

[4] Bose B. Modern Power Electronics and AC Drives. Prentice-Hall Inc., 2002, 738 p.

[5] Pressman A. I. Switching Power Supply Design. New York: McGraw-Hill, 2009. — 841 p.

[6] Shi L., Shan C., Wu X., Zhao N. Comparison of solid-state frequency converter and rotary frequency converter in 400HZ power system. International Conference on Electrical Machines and Systems, 2011, pp. 1 – 5. DOI: 10.1109/ICEMS.2011.6073791

[7] Taha M. H., Skinner D., Gami S., Holme M., Raimondi G. Variable frequency to constant frequency converter (VFCFC) for aircraft applications. International Conference on Power Electronics, Machines and Drives, 2002, pp. 235 – 240.

[8] Vinnychenko D., Nazarova N. Power converter adaptive control system of the installation for production of nanocarbons from gaseous hydrocarbons. IEEE 38th International Conference on Electronics and Nanotechnology (ELNANO), Kyiv, 2018, pp. 515 – 520. DOI: 10.1109/UKRCON.2017.8100307.

[9] Witulski A. F., Erickson R.W. Steady-state analysis of the series resonant converter. IEEE Trans. on Aerospace and Electronics Systems, 1985, vol. AES–21, No. 6, pp. 791 – 799.

Problem statement. To control the output voltage of the frequency converters people use effectively enough the pulse-density modulation technique [5 – 7]. However, the hard-switching operation mode of the pulse converter's power switches causes the significant switching losses, which can be reduced in the case of usage of the resonant commutation [3, 4, 8]. The combination of the resonant switching and pulse modulation principles will significantly reduce the switching losses of the power transistors and improve the converter electromagnetic compatibility with adjacent electronic devices and power network as well. The investigation of the electromagnetic processes in the power section of the frequency converter, which combines the advantages of pulse regulation and power transistors soft switching, is the topical task.

Latest research and publications analysis. The article [1], the authors analyzed the electromagnetic processes, which occur in the power section of the frequency converter, which forms a low-frequency output voltage by smoothing out the high-frequency pulses. The sinusoidal form of the pulses in that work was obtained due to the modeling results. However, in the cases of arbitrary circuit elements parameters, to provide the sinusoidal form of the carrier pulses and the form the pulse-density control pulses sequence, it is advisable to obtain analytical expressions for determining the duration of the inter-commutation stages in the converter circuits, in which the desired shape of the carrier pulses is provided. These expressions will subsequently allow formulating the control law, which will consider the non-sinusoidality of the certain sections of the carrier voltage pulses.

Thus, **THE ARTICLE AIM** is to study electromagnetic processes in the power section of the resonant frequency converter with pulse control and to obtain the analytical expressions for the durations of the inter-commutative stages of the converter operation.

Basic material. In fig. 1, a schematic diagram of the resonant frequency converter with pulse control is presented.

The circuit includes a DC link, which includes the diode bridge VD_{rec} and the filter capacitor C_{rec}. The resonant inverter executes the adjustment of the output voltage amplitude and frequency. It is a half-bridge, which includes the power transistors $VT1$ and $VT2$, and the serial resonant circuit $L_r – C_{r1}$ or $C_{r1} + C_{r2}$, and the low-frequency output filter $L_f – C_f$. the opposite diodes of the additional transistors $VT3$ and $VT4$ shunt the resonant capacitor. $VT3$ is switched on during the positive half-wave of the load voltage, and $VT4$ — during its negative half-wave. Since in the case of the parallel connection of the capacitors C_{r1} and C_{r2} and in the case of disconnection of the capacitor C_{r2} from the resonant circuit, the nature of the inverter behavior stays unaltered during one inter-commutation cycle, then they can be conventionally called C_r. And during the formation of the control sequence for the half-bridge switches, one should use the value $C_r = C_{r1} + C_{r2}$ or $C_r = C_{r1}$ depending on the state of the transistors VT5 and VT6.

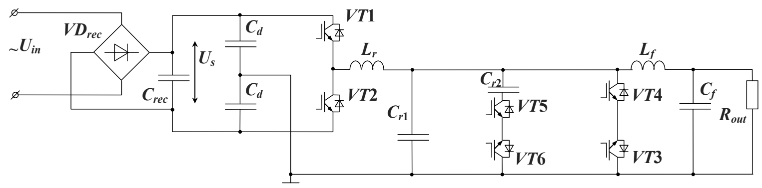

Fig. 1. Schematic diagram of the resonant frequency converter

When the control pulse occurs on the transistor $VT1$, the inductor L_r starts the energy accumulation. At the moment, when the current through L_r becomes equal to the current through L_f, the opposite diode of $VT3$ closes and the capacitor C_r starts charging. The current through L_r continues to grow until the voltage on C_r reaches the value $U_s/2$. The capacitor C_r charges to the value of U_s. At the moment, when the current through L_r reaches the value of the current through L_f, the C_r starts to discharge and its voltage falls according to the sinusoidal law. After the accumulated energy in the inductor L_r completely dissipates, the voltage of the capacitor C_r continues lowering linearly and when the voltage reaches zero, the opposite diode of the transistor $VT3$, which shunts the capacitor C_r, opens and the filter inductor L_f, which all that time is charging from the resonant circuit, starts to charge the filter capacitor C_f, which in turn supplies the load.

In the case of active load, due to the co-direction of the potential difference on the capacitor and the current through the filter inductor, the natural switching of one of the transistors $VT3$ or $VT4$ opposite diode occurs. Due to that, the current through the additional switch does not flow during the capacitor charging even in the case of a closed state of the corresponding additional transistor $VT3$ or $VT4$. In the case of the inductive load, the natural switching of the opposite diode does not occur, therefore, for the correct operation of the circuit it is necessary to carry out the forced switching of the corresponding additional transistor $VT3$ or $VT4$. The switches control signals can be described by the following logical equations:

$$U_{VT3} = (U_{out} > 0) \cdot (I_{out} \geq 0) \cdot \overline{U_{VT2}} + (U_{out} \leq 0) \cdot \\ \cdot (I_{out} > 0) \cdot \overline{U_{VT1}} \cdot \overline{U_{VT2}} \cdot \overline{U_{C\_rez}};$$

$$U_{VT4} = (U_{out} < 0) \cdot (I_{out} \leq 0) \cdot \overline{U_{VT1}} + (U_{out} \geq 0) \cdot \\ \cdot (I_{out} < 0) \cdot \overline{U_{VT1}} \cdot \overline{U_{VT2}} \cdot \overline{U_{C\_rez}}.$$

The investigation of the electromagnetic processes in the power section of resonant frequency converter, depending on the control parameter, can be conveniently carried out with the usage of the state-variable method [2, 9]. The equivalent circuit of the resonant inverter with pulse-density control are presented in fig. 2.

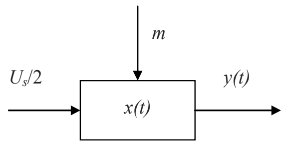

Fig. 2. The equivalent circuit of the resonant inverter with pulse-density control

The controlled variable here is the output voltage of the converter $y(t) = u_{out}(t)$. The input parameter here is the voltage $U_s/2$ on the half-bridge capacitors C_d. The control parameter here is the impulse ratio m, which is proportional to the frequency of the consecution of voltage pulses, which open one of the inverter power transistors during the output voltage positive half-wave, and the other one - during the negative half-wave. The processes, which occur in the power section of the converter, can be characterized by the state vector

$$\mathbf{x}^{\mathrm{T}}(t) = \left[i_{Lr}(t) \quad u_{Cr}(t) \quad i_{Lf}(t) \quad u_{Cf}(t) \right].$$

To describe the processes, which occur in the resonant inverter, consider one operation cycle, which can be conventionally divided into 5 stages. The equivalent diagrams for the power section of the converter during the inter-commutation stages $\Delta t_1 - \Delta t_5$ are shown in fig. $3, a-e$ respectively.

Differential equations, which describe the operation of the resonant inverter during 5 consecutive stages, have the following form:

a) for the first stage

$$\begin{cases} \dfrac{di_{Lr}}{dt} = -\dfrac{r_1 \cdot i_{Lr}}{L_r} + \dfrac{0{,}5U_s}{L_r}; \\ \dfrac{di_{Lf}}{dt} = -\dfrac{r_2 \cdot i_{Lf}}{L_f} - \dfrac{u_{Cf}}{L_f}; \\ \dfrac{du_{Cf}}{dt} = \dfrac{i_{Lf}}{C_f} - \dfrac{u_{Cf}}{R_{out} \cdot C_f}; \\ u_{Cf} = u_{out}. \end{cases}$$

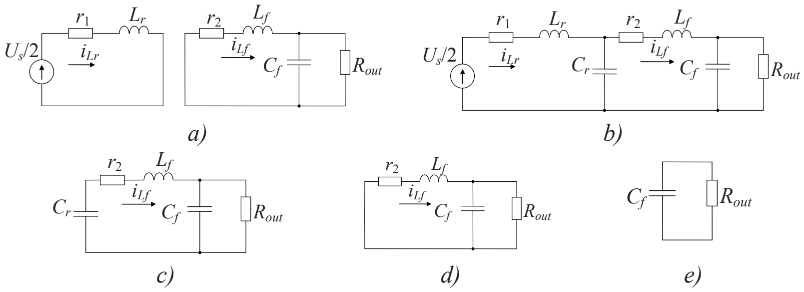

Fig. 3. The equivalent diagrams for the power section of the converter during the inter-commutation stages $\Delta t_1 - \Delta t_5$

b) for the first inter-commutation stage

$$\begin{cases} \dfrac{di_{Lr}}{dt} = -\dfrac{r_1 \cdot i_{Lr}}{L_r} - \dfrac{u_{Cr}}{L_r} + 0{,}5\dfrac{U_s}{L_r}; \\ \dfrac{du_{Cr}}{dt} = \dfrac{i_{Lr}}{C_r} - \dfrac{i_{Lf}}{C_r}; \\ \dfrac{di_{Lf}}{dt} = -\dfrac{i_{Lf} \cdot r_2}{L_f} - \dfrac{u_{Cf}}{L_f} + \dfrac{u_{Cr}}{L_f}; \\ \dfrac{du_{Cf}}{dt} = \dfrac{i_{Lf}}{C_f} - \dfrac{u_{Cf}}{R_{out} \cdot C_f}; \\ u_{Cf} = u_{out}. \end{cases}$$

c) for the third stage

$$\begin{cases} \dfrac{di_{Lf}}{dt} = -\dfrac{i_{Lf} \cdot r_2}{L_f} - \dfrac{u_{Cf}}{L_f} - \dfrac{u_{Cr}}{L_f}; \\ \dfrac{du_{Cf}}{dt} = \dfrac{i_{Lf}}{C_f} - \dfrac{u_{Cf}}{R_{out} C_f}; \\ u_{Cf} = u_{out}. \end{cases}$$

d) for the forth inter-commutation stage

$$\begin{cases} \dfrac{di_{Lf}}{dt} = -\dfrac{i_{Lf} \cdot r_2}{L_f} - \dfrac{u_{Cf}}{L_f}; \\ \dfrac{du_{Cf}}{dt} = \dfrac{i_{Lf}}{C_f} - \dfrac{u_{Cf}}{R_{out} C_f}; \\ u_{Cf} = u_{out}. \end{cases}$$

e) for the fifth inter-commutation stage

$$\begin{cases} \dfrac{du_{Cf}}{dt} = \dfrac{u_{Cf}}{R_{out} \cdot C_f}; \\ u_{out} = u_{Cf}. \end{cases}$$

In the vector-matrix form, these systems of equations will receive the following form:

a) for the first stage

$$\dot{\mathbf{x}}_1(t) = \mathbf{A}_1 \cdot \mathbf{x}_1(t) + \mathbf{B}_1 \cdot 0{,}5U_s; \; \mathbf{y}_1(t) = \mathbf{C}_1 \cdot \mathbf{x}_1(t); \quad (1)$$

b) for the second stage

$$\dot{\mathbf{x}}_2(t) = \mathbf{A}_2 \cdot \mathbf{x}_2(t) + \mathbf{B}_2 \cdot 0{,}5U_s; \; \mathbf{y}_2(t) = \mathbf{C}_2 \cdot \mathbf{x}_2(t); \quad (2)$$

c) for the third stage

$$\dot{\mathbf{x}}_3(t) = \mathbf{A}_3 \cdot \mathbf{x}_3(t) + \mathbf{B}_3 \cdot 0{,}5U_s; \; \mathbf{y}_3(t) = \mathbf{C}_3 \cdot \mathbf{x}_3(t); \quad (3)$$

d) for the forth stage

$$\dot{\mathbf{x}}_4(t) = \mathbf{A}_4 \cdot \mathbf{x}_4(t) + \mathbf{B}_4 \cdot 0{,}5U_s; \; \mathbf{y}_4(t) = \mathbf{C}_4 \cdot \mathbf{x}_4(t); \quad (4)$$

e) for the fifth stage

$$\dot{\mathbf{x}}_5(t) = \mathbf{A}_5 \cdot \mathbf{x}_5(t) + \mathbf{B}_5 \cdot 0{,}5U_s; \; \mathbf{y}_5(t) = \mathbf{C}_5 \cdot \mathbf{x}_5(t); \quad (5)$$

where

$$\mathbf{A}_1 = \begin{bmatrix} -\dfrac{r_1}{L_r} & 0 & 0 & 0 \\ 0 & 0 & 0 & 0 \\ 0 & 0 & -\dfrac{r_2}{L_f} & -\dfrac{1}{L_f} \\ 0 & 0 & \dfrac{1}{C_f} & 0 \end{bmatrix};$$

$$\mathbf{A}_2 = \begin{bmatrix} -\dfrac{r_1}{L_r} & -\dfrac{1}{L_r} & 0 & 0 \\ \dfrac{1}{C_r} & 0 & -\dfrac{1}{C_r} & 0 \\ -\dfrac{r_2}{L_f} & \dfrac{1}{L_f} & 0 & -\dfrac{1}{L_f} \\ 0 & 0 & \dfrac{1}{C_f} & -\dfrac{1}{R_{out} \cdot C_f} \end{bmatrix};$$

$$\mathbf{A}_3 = \begin{bmatrix} 0 & 0 & 0 & 0 \\ 0 & 0 & \frac{1}{C_r} & 0 \\ 0 & -\frac{1}{L_f} & -\frac{r_2}{L_f} & -\frac{1}{L_f} \\ 0 & 0 & \frac{1}{C_f} & -\frac{1}{R_{out} \cdot C_f} \end{bmatrix};$$

$$\mathbf{A}_4 = \begin{bmatrix} 0 & 0 & 0 & 0 \\ 0 & 0 & 0 & 0 \\ 0 & 0 & -\frac{r_2}{L_f} & -\frac{1}{L_f} \\ 0 & 0 & \frac{1}{C_f} & -\frac{1}{R_{out} \cdot C_f} \end{bmatrix};$$

$$\mathbf{A}_5 = \begin{bmatrix} 0 & 0 & 0 & 0 \\ 0 & 0 & 0 & 0 \\ 0 & 0 & 0 & 0 \\ 0 & 0 & 0 & \frac{1}{R_{out} \cdot C_f} \end{bmatrix};$$

$$\mathbf{B}_5 = \mathbf{B}_4 = \mathbf{B}_3 = \begin{bmatrix} 0 \\ 0 \\ 0 \\ 0 \end{bmatrix}; \ \mathbf{B}_1 = \mathbf{B}_2 = \begin{bmatrix} \frac{1}{L_r} \\ 0 \\ 0 \\ 0 \end{bmatrix};$$

$$\mathbf{C}_1 = \mathbf{C}_2 = \mathbf{C}_3 = \mathbf{C}_4 = \mathbf{C}_5 = \begin{bmatrix} 0 & 0 & 0 & 1 \end{bmatrix};$$

The matrixes $\mathbf{A}_{1-5}$ describe the circle topology, matrix $\mathbf{B}_{1-5}$ describe the connection of the source to the resonance circuit, matrixes $\mathbf{C}_{1-5}$ describe the directions of the currents in the circuit.

The solutions of the vector-matrix differential equations (1)–(5) are the following functions:

a) for the first stage

$$\mathbf{x}_1(t) = e^{\mathbf{A}_1 t} \cdot \mathbf{x}_1(0) + \int_0^t e^{\mathbf{A}_1(t-\tau)} \mathbf{B}_1 \cdot \mathbf{E} \cdot d\tau = $$
$$= e^{\mathbf{A}_1 t} \cdot \mathbf{x}_1(0) + \mathbf{A}_1^{-1}\left(e^{\mathbf{A}_1 t} - \mathbf{I}\right)\mathbf{B}_1 \mathbf{E}; \quad (6)$$

b) for the second stage

$$\mathbf{x}_2(t) = e^{\mathbf{A}_2(t-t_1)} \cdot \mathbf{x}_2(t_1) + \int_0^{t-t_1} e^{\mathbf{A}_2(t-t_1-\tau)} \mathbf{B}_2 \cdot \mathbf{E} \cdot d\tau =$$
$$= e^{\mathbf{A}_2(t-t_1)} \cdot \mathbf{x}_2(t_1) + \mathbf{A}_2^{-1}\left(e^{\mathbf{A}_2(t-t_1)} - \mathbf{I}\right)\mathbf{B}_2 \mathbf{E}; \quad (7)$$

c) for the third stage

$$\mathbf{x}_3(t) = e^{\mathbf{A}_3(t-t_2)} \cdot \mathbf{x}_3(t_2) + \int_0^{t-t_2} e^{\mathbf{A}_3(t-t_2-\tau)} \mathbf{B}_3 \cdot \mathbf{E} \cdot d\tau =$$
$$= e^{\mathbf{A}_3(t-t_2)} \cdot \mathbf{x}_3(t_2) + \mathbf{A}_3^{-1}\left(e^{\mathbf{A}_3(t-t_2)} - \mathbf{I}\right)\mathbf{B}_3 \mathbf{E} =$$
$$= e^{\mathbf{A}_3(t-t_2)} \cdot \mathbf{x}_3(t_2); \quad (8)$$

d) for the forth stage

$$\mathbf{x}_4(t) = e^{\mathbf{A}_4(t-t_3)} \cdot \mathbf{x}_4(t_3) + \int_0^{t-t_3} e^{\mathbf{A}_4(t-t_3-\tau)} \mathbf{B}_4 \cdot \mathbf{E} \cdot d\tau =$$
$$= e^{\mathbf{A}_4(t-t_3)} \cdot \mathbf{x}_4(t_3) + \mathbf{A}_4^{-1}\left(e^{\mathbf{A}_4(t-t_3)} - \mathbf{I}\right)\mathbf{B}_4 \mathbf{E} =$$
$$= e^{\mathbf{A}_4(t-t_3)} \cdot \mathbf{x}_4(t_3); \quad (9)$$

e) for the fifth stage

$$\mathbf{x}_5(t) = e^{\mathbf{A}_5(t-t_4)} \cdot \mathbf{x}_5(t_4) + \int_0^{t-t_4} e^{\mathbf{A}_5(t-t_4-\tau)} \mathbf{B}_5 \cdot \mathbf{E} \cdot d\tau =$$
$$= e^{\mathbf{A}_5(t-t_4)} \cdot \mathbf{x}_5(t_4) + \mathbf{A}_5^{-1}\left(e^{\mathbf{A}_5(t-t_4)} - \mathbf{I}\right)\mathbf{B}_5 \mathbf{E} =$$
$$= e^{\mathbf{A}_5(t-t_4)} \cdot \mathbf{x}_5(t_4). \quad (10)$$

The resonant circuit current and voltage curves required for calculating the time for each inter-commutative stage are shown in fig. 4.

Since the operation cycle of the resonant inverter is conditionally divided into 5 successive inter-commutative stages, with the final conditions at each of the stages being initial for the further, then to determine the moments of the beginning and end of each of the stages, it is necessary to determine their duration, which are as follows:

a) the duration of the first stage

$$\Delta t_1 = \frac{2 i_{Lf}(t_0) \cdot L_r}{U_s}, \quad (11)$$

where $i_{Lf}(t_0)$ — instantaneous value of the current through the filter inductor at the moment of the control pulse start, L_r — resonant inductance, U_s — inverter input direct voltage.

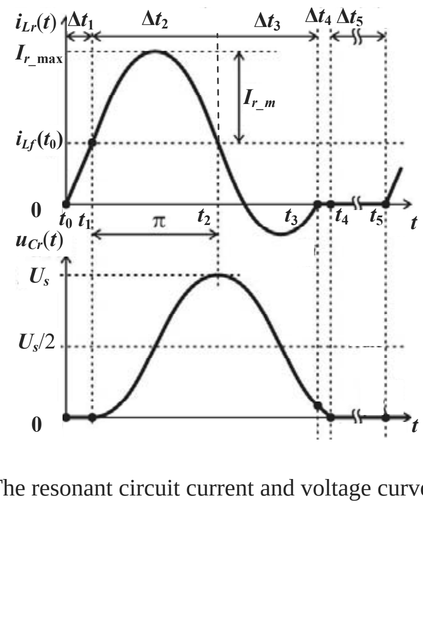

Fig. 4. The resonant circuit current and voltage curves

b) the duration of the second stage

$$\Delta t_2 = \frac{T_r}{2} + \frac{\arcsin\left(i_{Lf}(t_0)/I_{r\_m}\right)}{\omega_r}; \qquad (12)$$

where I_{r_m} — resonant current amplitude, T_r — resonant period, $\omega_r = 2\pi/T_r$ — natural frequency of the resonant circuit.

c) the duration of the third stage

$$\Delta t_3 = \frac{T_r}{2} - \frac{2\arcsin\left(i_{Lf}(t_0)/I_{r\_m}\right)}{\omega_r}; \qquad (13)$$

d) the duration of the forth stage

$$\Delta t_4 = \frac{U_s}{2}\left[1-\cos\left(\omega_r\left[T_r - \frac{\arcsin(i_{Lf}(t_0)/I_{r\_m})}{\omega_r} + \frac{2i_{Lf}(t_0)L_r}{U_s}\right]\right)\right]\cdot\frac{C_r}{i_{Lf}(t_0)}; \qquad (14)$$

e) the duration of the fifth stage

$$\Delta t_5 = t_i - t_4 . \qquad (15)$$

Based on the obtained stages durations (11)–(15), end moments of each inter-commutation stage are obtained as follows. The end moment of the first conditional stage:

$$t_1 = t_0 + \frac{2i_{Lf}(t_0)\cdot L_r}{U_s}. \qquad (16)$$

The end moment of the second inter-commutation stage:

$$t_2 = t_0 + t_1 + \frac{T_r}{2} + \frac{\arcsin\left(i_{Lf}(t_0)/I_{r\_m}\right)}{\omega_r}. \qquad (17)$$

The end moment of the third inter-commutation stage:

$$t_3 = t_0 + T_r - \frac{\arcsin\left(i_{Lf}(t_0)/I_{r\_m}\right)}{\omega_r} + \frac{2i_{Lf}(t_0)L_r}{U_s}. \qquad (18)$$

The end moment of the forth inter-commutation stage:

$$t_4 = t_1 + \Delta t_2 + \Delta t_3 + \Delta t_4. \qquad (19)$$

The end moment of the fifth inter-commutation stage:

$$t_5 = t_i. \qquad (20)$$

Fig. 5 shows the theoretical (*a*) and experimental (*b*) phase diagrams of the pulse-regulated resonant inverter operation cycle, constructed on the basis of the solutions of the differential equations systems (6)–(10).

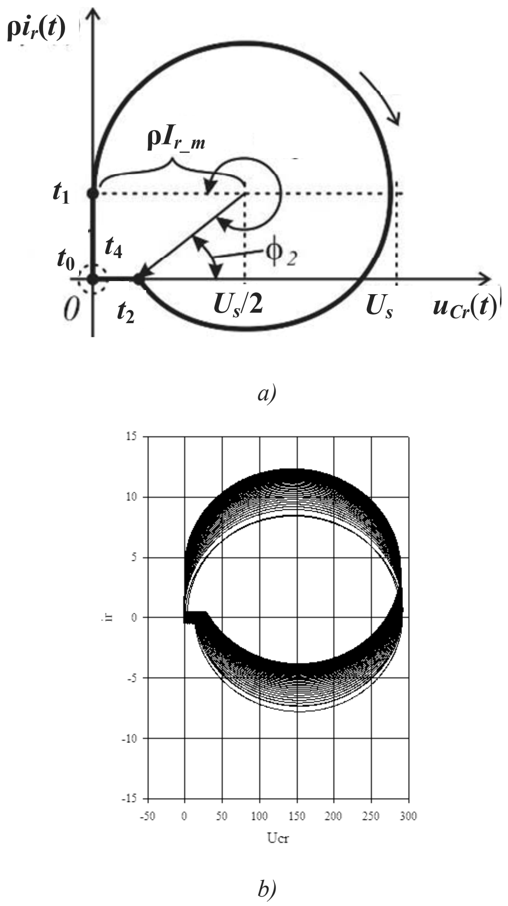

Fig. 5. The theoretical (*a*) and experimental (*b*) phase diagrams of the pulse-regulated resonant inverter operation cycle

The obtained phase diagrams allow visualizing the electromagnetic processes, which occur in the power section of the frequency converter. Due to the constructed mathematical model, the exact form of the carrier pulses was gotten and the durations of the stages, in which one can receive the desired form of carrier sinusoidal voltage pulses with the low THD, were determined.

The simulation model (Fig. 6) of the resonant inverter was constructed. The parameters of the model are as follows: the capacitance of the resonant capacitors C_{r1} = 5 nF and C_{r2} = 5 nF, the inductance of the resonant coil L_r = 12 μG, the filter inductance L_f = 0.33 mH, the filter capacitance C_f = 1.8 μF.

The control system generates the output sinusoidal voltage according to the pulse-density law. The switching of all inverter transistors is carried out in a way as to ensure the duration of the inter-commutation stages calculated according to (16)–(20). The simulation results are shown in Fig. 7. Fig. 7,*a* shows the resonant current pulses sequence, the sequence of the carrier resonant voltage pulses, and a low-frequency load voltage. In fig. 7,*b* the resonant current and voltage pulses of the enlarged scale are depicted.

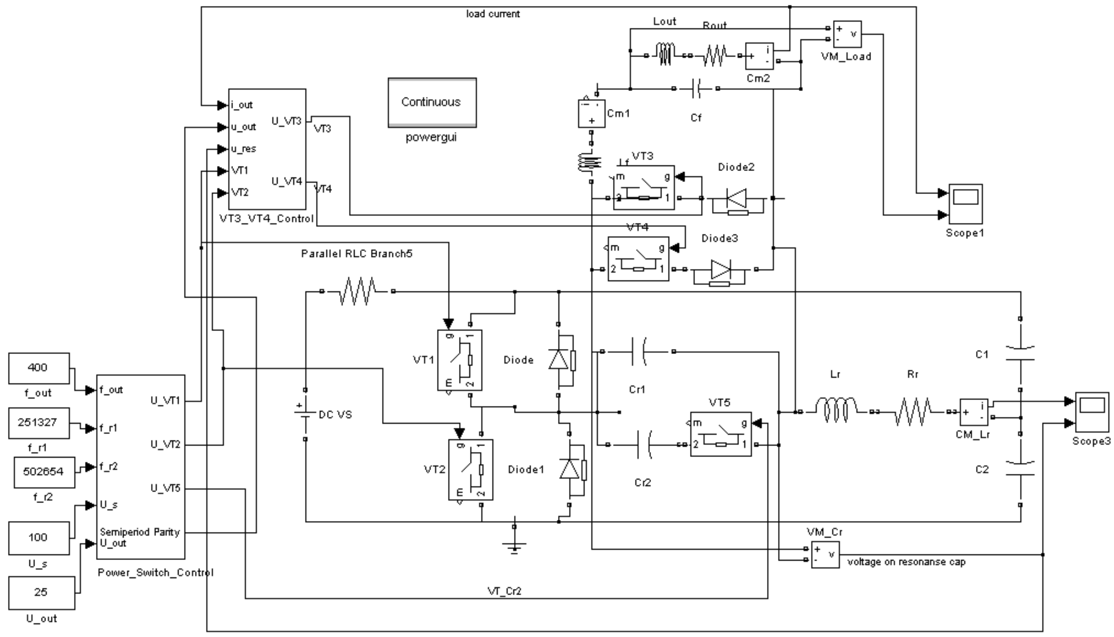

Fig. 6. Simulation model of the resonant inverter

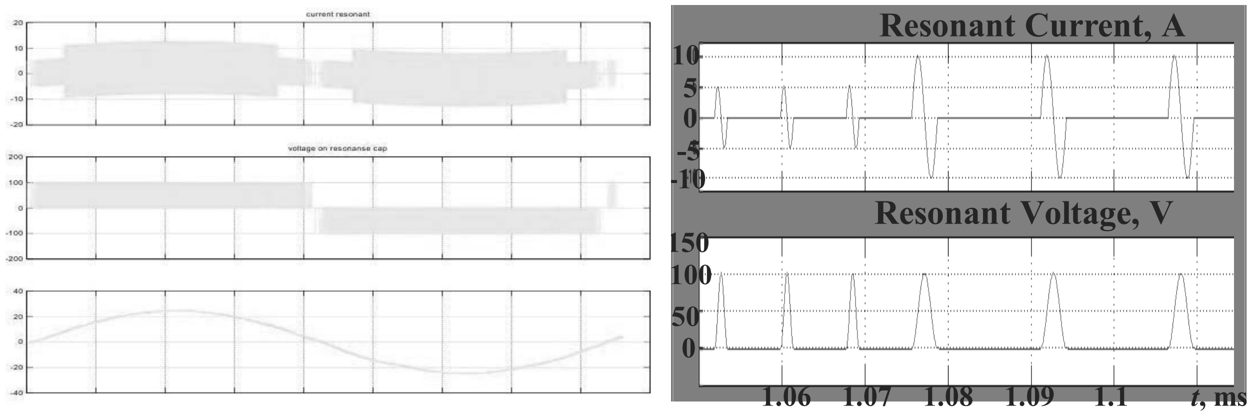

a) *b)*

Fig. 7. The resonant converter simulation results

The spectrum of the carrier resonant capacitor voltage pulses is shown in fig. 8, *a*, which corresponds to the total harmonic distortion value of THDV = 2.01 %. The spectrum of high-frequency resonance coil current pulses is shown in Fig. 8, *b*. Their total harmonic distortion is 1.07 %.

Thus, the formation of the frequency converter power switches control pulses durations and sequence, which allow providing the chain of inter-commutation stages mentioned in the paper, leads to obtaining the desired piecewise-sinusoidal shape of the carrier resonant voltage and current pulses with the low values of the total harmonic distortions.

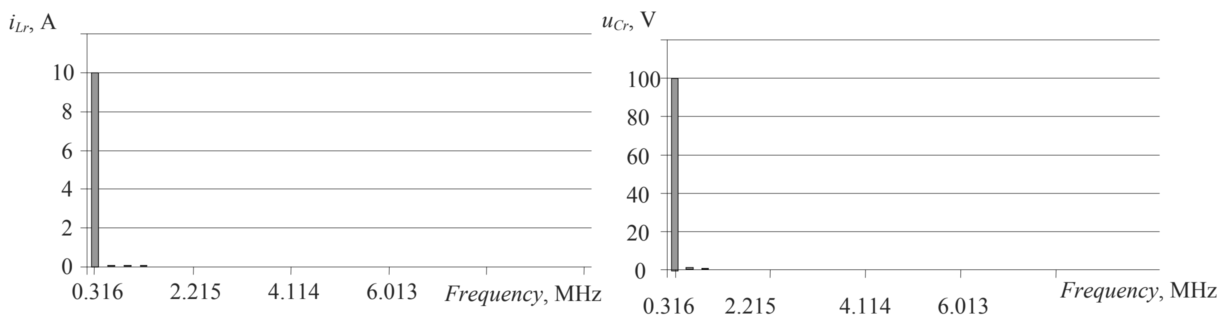

a) *b)*

Fig. 8. The spectrum of the resonant current (*a*) and voltage (*b*) pulses

CONCLUSIONS. Thus, the analytical expressions for calculating the durations (11)–(15) of the inter-commutation stages and their end moments (16)–(20) are obtained. They allow calculating the switching moments for the converter power transistors in order to provide the sinusoidal shape of carrier voltages pulses and resonant current pulses with low total harmonic distortion (2.01% and 1.07% respectively). Based on the mathematical model of the converter, the converter operational cycle computed and experimental phase diagrams are received and the electromagnetic processes occurring in the power section of the resonant frequency converter, which work involves the combination of the soft switching and output voltage pulse regulation principles, were analyzed. The computer simulation of the resonant frequency converter operation is implemented. It presumed the carrier pulses generation by real time calculating the power transistors switching moments in accordance with (16)–(20) and the described algorithm that allowed analyzing the spectra of the carrier voltage and current pulses, and confirming the obtained theoretical results.

Список литературы

[1] **Павлов, Г. В.** Электромагнитные процессы и параметры накопительных элементов в резонансном инверторе с нелинейным регулированием [Текст] / Г. В. Павлов, А. В. Обрубов, И. Л. Винниченко / «Судостроение и морская инфраструктура». — Николаев : НУК, 2015. — №2(4). — С. 96–107.

[2] **Сигорский, В. П.** Математический аппарат инженера [Текст] / В. П. Сигорский. — К.: «Техніка», 1977. — 768 с.

[3] **Юрченко, О. М.** Модель резонансного транзисторного інвертора напруги з низькочастотною імпульсною модуляцією / О. М. Юрченко, В. Я. Гуцалюк, П. Ю. Герасименко, І. О. Слєсаревський // «Технічна електродинаміка» № 1, 2011. — С. 24–30.

[4] **Bose, B.** Modern power electronics and AC drives [Text] / Bimal Bose. Prentice-Hall Inc., 2002, 738 p.

[5] **Pressman, A. I.** Switching power supply design [Text] / A. I. Pressman, K. Billings, T. Morey. — New York: McGraw-Hill, 2009. — 841 p.

[6] **Shi, L.** Comparison of solid-state frequency converter and rotary frequency converter in 400 Hz power system / L. Shi, C. Shan, X. Wu, N. Zhao // International Conference on Electrical Machines and Systems, 2011. — pp. 1–5. DOI: 10.1109/ICEMS.2011.6073791

[7] **Taha, M. H.** Variable frequency to constant frequency converter (VFCFC) for aircraft applications [Text] / M. H. Taha, D. Skinner, S. Gami, M. Holme, G. Raimondi // International Conference on Power Electronics, Machines and Drives, 2002. — pp. 235–240.

[8] **Vinnychenko, D.** Power Converter Adaptive Control System of the Installation for Production of Nanocarbons from Gaseous Hydrocarbons [Text] / D. Vinnychenko, N. Nazarova // "IEEE 38th International Conference on Electronics and Nanotechnology (ELNANO)". — Kyiv, 2018, — pp. 515–520. DOI: 10.1109/UKRCON.2017.8100307.

[9] **Witulski, A. F.** Steady-state analysis of the series resonant converter [Text] / Witulski A.F., Erickson R.W. // IEEE Trans. on Aerospace and Electronics Systems, 1985. — Vol. AES-21, No.6. — pp. 791–799.

Статтю рекомендує до друку
д-р техн. наук, проф. *Н. І. Кускова*